

Large scale PIV-measurements on the water surface of turbulent open-channel flow

Albayrak Ismail & Lemmin Ulrich

*Ecole Polytechnique Fédérale de Lausanne
Laboratory of Environmental Hydraulics (LHE)
Station 18, CH-1015 Lausanne, Suisse / Switzerland
ismail.albayrak@epfl.ch & ulrich.lemmin@epfl.ch*

Abstract :

An experimental open-channel laboratory study of secondary currents and surface boils is presented. Surface velocity dynamics over a large measuring field were investigated using Large Scale Particle Image Velocimetry (LSPIV). Data were analyzed for the structures of the large streamwise vortices and surface boils. The results indicate a mean multi-cellular pattern of faster and slower primary longitudinal velocities. The mean transversal velocities show a corresponding pattern. The spacing of the surface pattern of upwelling and downwelling is related to the water depth. The instantaneous pattern of the secondary currents meanders around the mean pattern. Vortex boils occur near the upwelling regions. Details of the vortex structures, in particular the growth and spreading of individual vortices when moving along the flow, are detected from instantaneous velocity maps of the water surface using a moving-camera PIV which follows the flow at the mean surface current speed.

Résumé :

Une étude des courants secondaires et des bouffées turbulentes à la surface libre dans un canal ouvert de laboratoire est décrite. La dynamique des vitesses de surface pour une grande surface de mesures est étudiée en utilisant un "Large Scale Particle Image Velocimetry (LSPIV)". Les données ont été analysées pour les structures de grands vortex dans la direction de l'écoulement et pour les bouffées à la surface. Les résultats montrent des structures multi-cellulaires moyennes à des vitesses plus grandes et plus petites que la vitesse longitudinale principale. Les vitesses moyennes transversales montrent des structures correspondantes. L'espacement des structures de surface d'upwelling et downwelling est relié à la profondeur d'eau. Les structures instantanées des courants secondaires sinuent autour de la structure moyenne. Des bulles de vortex ont lieu près des régions d'upwelling. Des détails des structures des vortex, en particulier la croissance et l'étalement de vortex individuels durant leurs mouvements le long du courant sont détectés à partir des cartes de vitesses instantanées de la surface d'eau en utilisant une camera PIV mobile qui suit le courant avec la vitesse du courant de surface.

Key-words : Surface PIV; secondary currents; surface boils.

1 Introduction

Exchange processes at the air-water interface have been the subject of many studies related to effective water resource management, river engineering and environmental fluid mechanics. Turbulence structures close to the free surface such as 'upwelling', 'downwelling' or 'spiral eddies' may significantly influence the transfer of oxygen, carbon dioxide, heat and momentum and self-aeration dynamics. These processes are of significance for the long-term development of the ecosystem and may be affected by climate dynamics. Surface boils observed on rivers are important in the air-water gas exchange.

Turbulence structures generated by shear at the bottom of a channel flow and their effect at the free-surface have been the subject of a number of studies (Komori et al., 1989, Kumar et al., 1998 and Tamburrino and Gulliver, 1999). Kumar et al. (1998) presented an extensive investigation of free-surface turbulence in open-channel flow using HDPIV measurement techniques at the surface. They classified the persistent structures of the free surface as upwellings, downdrafts and spiral eddies. It was shown that at

low Reynolds numbers, upwellings were related to bursts originating in the sheared region of the water column near the channel bottom and surface eddies were generated at the edges of these upwellings. DNS results from Pan and Banerjee (1995) were in good agreement with these experiments.

Surface boils occur in many free surface flows, and are best documented for rivers. Nezu and Nakagawa (1993) suggested three different mechanisms for the generation of surface boils. Their 'boils of the second kind' are associated with cellular secondary currents and are seen in wide, straight rivers. They point out that fairly stable boil lines are formed at the surface between two neighboring secondary current cells. Tamburrino et al. (1999) observed that large streamwise vortices scale with flow depth and create upwelling and downwelling motions. Boils and eddies with a vertical axis are detected in upwelling zones. Moog and Jirka (1999) studied the effect of surface boils on air-gas exchange in detail. They concluded that in turbulent flows, surface boils contribute to river re-aeration and affect water quality management concepts.

The primary goal of this study is to investigate experimentally free surface turbulence structures such as secondary currents and surface boils as well as the interaction between them in open-channel flow. Large Scale Particle Image Velocimetry (LSPIV) techniques were used to extract surface skin velocity maps from video images which allow quantifying the velocity field. In the first part of this paper, the experimental set-up, procedure and instrumentation are described. In the second part, the mean velocity profiles across the water surface obtained with LSPIV are analyzed with respect to secondary currents and surface boils. Thereafter, vortex visualizations and moving camera measurements are presented in order to examine the relationship between surface boils and upwelling structures.

2 Experimental set-up and procedure

The experiments were conducted in the 2.4 m wide, 20 cm deep and 27 m long open-channel of the LHE (Fig. 1). The aspect ratio B/h was equal to 12.25 (Table 1). The bed of this channel consists of mixed gravel, whose size ranges from 10 mm to 20 mm. Fully developed uniform flow was established at about 15 m from the entrance of the channel. The discharge was always below the threshold for bed particle motion. Three experiments were conducted at three different Reynolds numbers ranging from 29.5 to $106.8 \cdot 10^3$ (Table 1). Further experimental conditions are summarized in Table 1.

Exp.	Q m ³ /s	h cm	U m/s	U_{max} m/s	U_* cm/s	Re_h	Fr_h	B/h	d_{50} cm
1	0.257	19.5	0.55	0.73	4.18	$106.8 \cdot 10^3$	0.3977	12.25	1.5
2	0.185	19.5	0.3954	0.54	2.83	$76.99 \cdot 10^3$	0.2856	12.25	1.5
3	0.07	19.5	0.152	0.21	0.97	$29.5 \cdot 10^3$	0.1099	12.25	1.5

Table 1: Hydraulic parameters for experiments

2.1 Large Scale Particle Image Velocimetry (LSPIV)

A PIV system was developed in order to visualize the water surface flow field. It consists of illuminating the free surface, seeding it with small light-reflective white particles with an in-house developed 'spreading machine', recording short time exposure images of a limited area of the water surface and processing the recorded video data.

The particles were floating Polypropylene cylinders (1-2 mm) corresponding to 2.1 pixels per particle and were coated to minimize agglomeration effects. An ideal particle size should be between 1.5 to 5 pixels in order to overcome problems of peak-locking effects and of not following the flow structures (Weitbrecht et al., 2002). The bottom of the channel was painted black to provide sufficient contrast with the white particles.

A particle spreading machine similar to the one described in Weitbrecht et al. (2002) was developed at the LHE to provide a homogeneous distribution of the particles on the water surface and placed close to the measurement field (Fig. 1). A CDD camera with a resolution of 720 x 576 pixels operating at 25 fps was used to record a 30x60 cm area of the water surface (Fig. 2). Two LSPIV measurements on the water surface were carried out side-by-side across the channel in order to cover one half of the flume width. Video files recorded for 3 min at each position were transferred to the computer for further analysis.

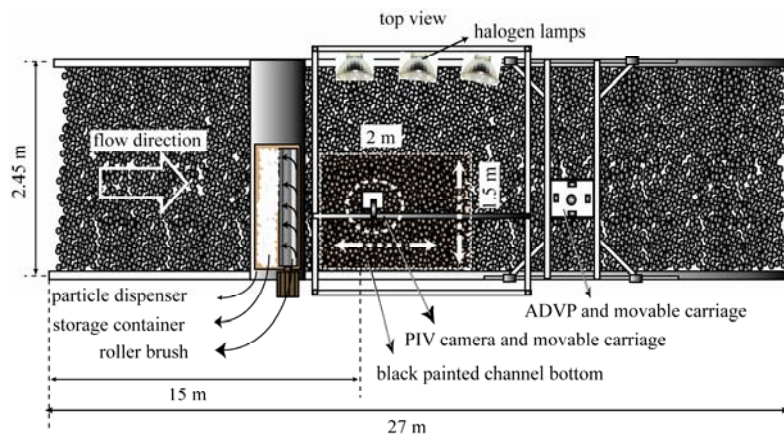


FIG 1. Schematic diagram of the hydraulic flume and test section

The LSPIV system uses PIV software, image processing software and a high performance PC. A PIV software based on a standard cross correlation between two consecutive images using FFT (Raffel et al.1998) was adapted to our specific conditions of data interpretation particularly related to vortex dynamics. For the large surface areas covered in these experiments, a wide-angle optic lens was used. In order to correct the distorted images obtained with this lens, a small program was developed and added to the main PIV software. Adaptive multi-pass processing was used due to the high dynamic range of the velocities in open-channel flows. The PIV software starts with the selected interrogation window (64x64 pixels in this case) and uses the calculated velocity as the reference velocity for the next smaller interrogation window. After this calculation, the velocity data are filtered with a signal-to-noise filter, a peak height filter, and global and local filters in order to remove error vectors.

Subsequently, moving camera PIV measurements were conducted for experiment 3 at the low Reynolds number (Table 1). A movable carriage holding the CCD camera was mounted above the channel in order to follow individual surface flow structures. The carriage speed was adjusted so that the camera moved along the channel with the velocity of the water surface.

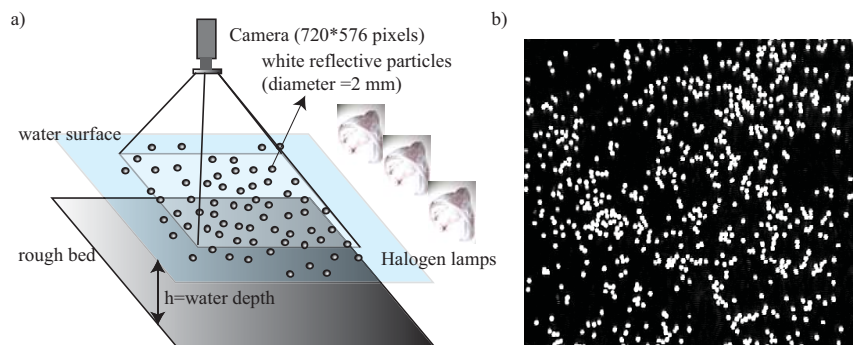


FIG. 2 (a) Sketch of the LSPIV system (b) PIV image from experiment 3.

3 Results

3.1 Mean surface velocity pattern

The mean longitudinal and transversal velocity patterns are shown in Fig. 3. The undulation of the longitudinal mean velocity indicating systematically organized faster and slower moving zones can be seen in Fig. 3a. The difference between the maximum and the minimum velocity is about 10% which corresponds to previous observations. The velocity differences can be related to upwelling and downwelling structures in the water column. This pattern can be explained by stationary secondary currents (Nezu, 2005). The spacing between the cells is close to the water depth, as would be expected.

From Fig. 3b, three stationary secondary cell pairs can be identified. However, towards the center of the channel, secondary cells lose their strength and show weaker transversal velocities. This may be explained by the observed instability and lateral shift of the secondary currents close to the center of channel at higher Reynolds numbers.

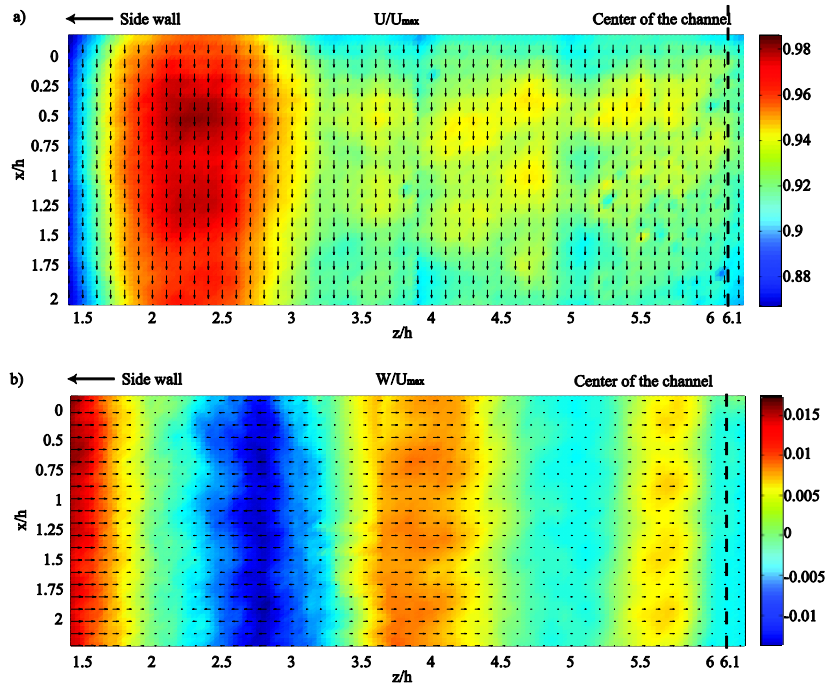


FIG. 3 Mean pattern (three minutes) of (a) downstream and (b) transversal velocity obtained from surface PIV measurements.

3.2 Vortex visualization

A technique based on choosing a reference frame moving with a convection velocity U_c was used to decompose the velocity field in order to detect flow structures such as vortices, swirling and upwelling on the water surface. Details of the technique can be found in Adrian et al. (2000). A vortex is defined as a region of concentrated vorticity around which the pattern of streamlines is roughly circular when viewed in a frame moving with the center of the vortex. Increasing and decreasing the convection velocity in small increments can identify different vortices. Here, $U_c = 0.90U_{max}$ was used as the convection velocity.

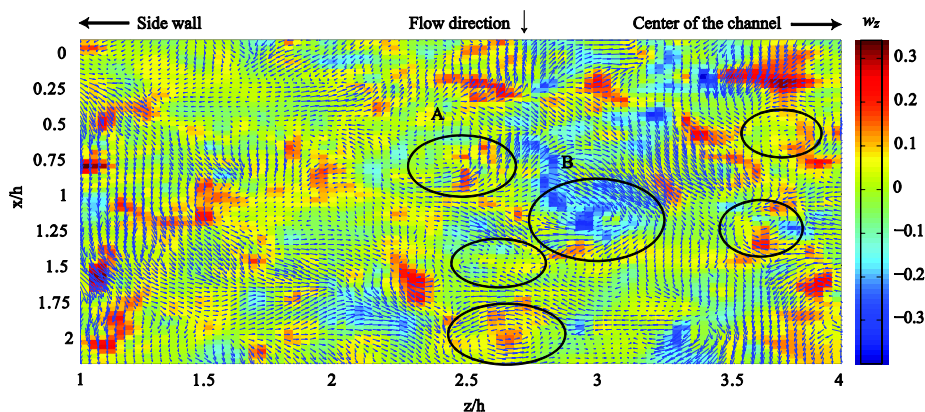


FIG. 4 Surface normal PIV measurement of instantaneous velocity (vectors) and vorticity field (background). Vectors are viewed in a reference frame, convecting with $U_c = 0.90U_{max}$.

Vorticity was calculated using the equation $w_z = dw/dx - du_s/dz$, $u_s = u - U_c$. The instantaneous flow velocity field after subtracting the convection velocity and the vorticity field in the background are shown in Fig. 4. The vectors have negative longitudinal components around $z/h=3.2$ corresponding to the upwelling region with slower mean longitudinal velocity (Fig. 3a) whereas they have positive longitudinal components at around $z/h= 1.5-2$ and $3.5-4$, which indicates downwelling zones (Fig. 3a). Due to the strong velocity gradient between the side wall and $z/h=2$, there are stronger negative longitudinal velocity vectors. As seen from Fig. 4b, the cores of two vortices labeled A and B roughly coincide with a concentration of negative and positive vorticity respectively. They produce a circular streamline pattern, because the convection velocity matches the velocity of the vortex centers. The vortex pair A, B and several other vortices form a vortex street in an upwelling zone. In our study, the size of individual vortices varies, but does not exceed the water depth, h . For a higher Reynolds number flow, Tamburroni and Gulliver (1989) indicated that secondary currents create vortex streets in upwelling zones which agrees well with the present results.

3.3 PIV results from the moving camera experiment

In order to further elucidate the dynamics of vortex formation, PIV measurements were conducted for experiment 3 by moving the camera along the channel at the mean surface flow speed, which allows following the development of the same surface area of the flow for up to 10 sec. A typical result is plotted in Fig. 5. It can be seen that upwelling is produced locally and that the patch, identified as the region free of particles, grows in time, thus indicating that the development of the patch occurs over a significant time period during which the vortex does not change its relative position. In this case the velocity vectors are mainly outwards oriented around the patch. However, the formation of patches with vertical motion around the rim was also observed. An upwelling patch coming up to the water surface was observed to generate one or more smaller vortices at the edge of the upwelling (Fig. 5) thus revealing the typical generation of spiral eddies in upwelling zones as shown in the study by Kumar et al. (1998). The development presented in Fig. 5 points towards the importance of individual coherent structures in the

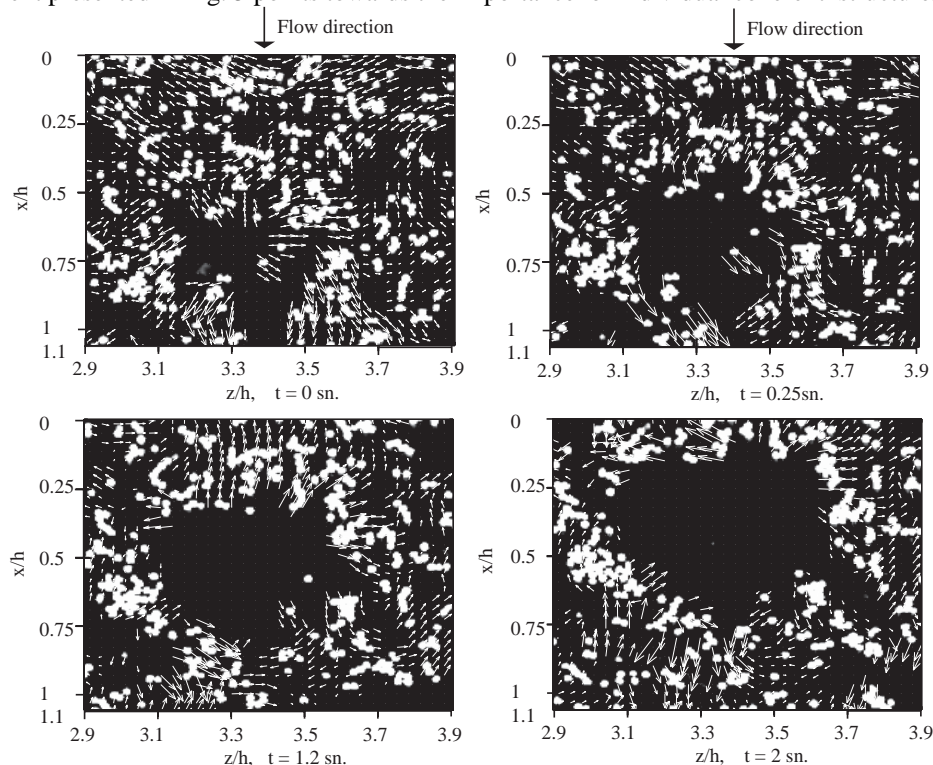


FIG. 5 PIV results of instantaneous surface velocities obtained with the moving video camera

water column for the formation of the surface flow pattern. Our analysis of water velocity data (not shown here) indicates that there are almost 10% more ejections in the upwelling zones than in the downwelling zones in the upper water column. This distribution can explain the observed vortex pattern.

4 Conclusions

Surface PIV measurements of turbulent open-channel flows were carried out in order to investigate the effects of processes in the water column on the dynamics of free surface flow. Three different sets of PIV measurements revealed a clear surface pattern of secondary currents of a second kind. The long-term temporal average of large streamwise vortices in the water column results in relatively stable secondary currents of alternating sense of rotation scaling with water depth. Stable large streamwise vortices always occur close to the sidewall and their successive superposition generates secondary currents in the long term. At high Reynolds numbers, secondary currents are continuously shifting at the center of channel. The number of secondary current cells is independent of the Reynolds number. It is found that upwelling regions on the water surface have lower longitudinal mean water velocity. Downwelling regions are recognized as streaks with higher longitudinal mean velocity and lower vorticity. Vortex structures are detected from the instantaneous velocity map of water surface obtained by using a reference frame technique and from moving camera PIV measurements. Vortex visualization experiments show vortical motions with a vertical axis. They are mainly associated with upwelling regions of the secondary currents. Vortex size is roughly equal to a water depth. Moving camera results show the growth of upwelling patches.

Surface boils are generated in the upwelling zones and play a key role in surface renewal and for gas exchange. Our measurements have shown that up- and downwelling as well as surface boils occur over a wide range of Reynolds numbers and can therefore be considered important processes in river dynamics.

Acknowledgements

We are grateful for the financial support that was provided by the Swiss National Science Foundation, grant 200020-100383, for this study.

References

- Gulliver, J. S. & Halverson, M. J. 1989 Air-water gas transfer in open channels. *Water Resour. Res.*, **25**, 1783-1793.
- Komori, S., Murakami, Y. & Ueda, H. 1989 The relationship between surface-renewal and bursting motions in an open-channel flow. *J. Fluid Mech.* **203**, 103-123.
- Kumar, S., Gupta, R. & Banerjee, S. 1998 An experimental investigation of the characteristics of free-surface turbulence in channel flow. *Phys. Fluids* **10**, 437-456.
- Moog, D. B. & Jirka, G. H. 1999 Air-water gas transfer in uniform channel flow. *J. Hydraul. Eng. ASCE* **125**, 3-10.
- Nezu, I. & Nakagawa, H. 1993 Turbulence in open-channel flows. IAHR Monograph series.
- Nezu, I. 2005 Open-channel flow turbulence and its research prospect in the 21. century. *J. Hydraul. Eng. ASCE* **131**, 229-246.
- Pan, Y. & Banerjee, S. 1995 Numerical investigation of free-surface turbulence in open-channel flows, *Phys. Fluids* **7**, 1649.
- Raffel, M., Willert, C. E. & Kompenhans, J. 1998 Particle Image Velocimetry. Springer Berlin.
- Tamburrino, A. & Gulliver, J. S. 1999 Large flow structures in a turbulent open channel flow. *J. Hydraul. Res.* **37**, 363-380.
- Weitbrecht, V., Kühn, G. & Jirka, G. H. 2002 Large scale PIV-measurements at the surface of shallow water flows. *Flow Measurement and Instrumentation* **13**, 237-245.